Energy Efficiency Analysis and Optimization for Virtual-MIMO Systems

Jing Jiang, *Member, IEEE,* Mehrdad Dianati, *Member, IEEE,*
Muhammad Ali Imran, *Senior Member, IEEE,*
Rahim Tafazolli, *Senior Member, IEEE,* Shunqing Zhang, *Member, IEEE.*

Abstract

Virtual multiple-input multiple-output (MIMO) systems using multiple antennas at the transmitter and a single antenna at each of the receivers, have recently emerged as an alternative to point-to-point MIMO systems. This paper investigates the relationship between energy efficiency (EE) and spectral efficiency (SE) for a virtual-MIMO system that has one destination and one relay using compress-and-forward cooperation. To capture the cost of cooperation, the power allocation (between the transmitter and the relay) and the bandwidth allocation (between the data and cooperation channels) are studied. This paper derives a tight upper bound for the overall system EE as a function of SE, which exhibits a good accuracy for a wide range of SE values. The EE upper bound is used for formulating an EE optimization problem. Given a target SE, the optimal power and bandwidth allocation can be derived such that the overall EE is maximized. Results indicate that the EE performance of virtual-MIMO is sensitive to many factors including resource allocation schemes and channel characteristics. When an out-of-band cooperation channel is considered, the performance of virtual-MIMO is close to that of the MIMO case, in terms of EE. Considering a shared-band cooperation channel, virtual-MIMO with optimal power and bandwidth allocation is more energy efficient than the non-cooperation case, under most SE values.

Index Terms

Energy efficiency, Virtual MIMO system, CF cooperation, Power allocation, Fading channels.

J. Jiang, M. Dianati, M. A. Imran and R. Tafazolli are with the Centre for Communication Systems Research, Department of Electronic Engineering, University of Surrey, GU2 7XH, Surrey, U.K. (Email: {Jing.Jiang, M.Dianati, M.Imran, R.Tafazolli}@surrey.ac.uk)

S. Zhang is with Huawei Technologies, Co. Ltd., Shanghai, China. (Email: sqzhang@huawei.com)

I. INTRODUCTION

Virtual multiple-input multiple-output (MIMO) systems, where the transmitter has multiple antennas and each of the receivers has a single antenna, have recently emerged as an effective technique that can improve the spectral efficiency of wireless communications [1] [2]. The idea is that when channel state information (CSI) is available at the receiver side only, some neighbor receivers can contribute their antennas (i.e., serve as relays) and help the single-antenna destination to form a virtual antenna array and to reap some of the benefits of MIMO systems [3], [4]. Virtual-MIMO is a promising idea for terrestrial mobile communication systems as some mobile stations in these systems may not be equipped with multiple antennas due to their physical constraints.

Most of the previous work on virtual-MIMO systems has focused on spectral efficiency (SE) and bit error ratio performance, such as [2], [4], and [5]. It has been shown that cooperation among receivers can enhance the efficiency of frequency spectrum utilized, compared to the non-cooperative multiple-input and single-output (MISO) systems. However, the SE metric fails to provide any insight on how efficiently energy is consumed. The impact of cooperation, considering a realistic model that takes into account both transmit and circuit energy consumption at the transmitter and relay nodes, on the overall energy efficiency (EE) of the system has not yet been adequately studied, to the best of our knowledge. In addition, maximizing the EE, or equivalently minimizing the total consumed energy, while maximizing the SE are generally conflicting objectives; but they can be linked together and balanced through their relationship [6]. That is, for certain values of SE, whether and under what conditions cooperation at the receiver side can offer benefits in terms of overall EE, when a realistic energy consumption model is considered. This is a particularly important question for network operators and telecommunication equipment manufacturers as there is a global demand for future wireless networks to become more energy efficient [7]–[9].

Essentially virtual-MIMO can be viewed as a combination of MIMO and cooperation technologies. From the cooperation perspective, the relay node in virtual-MIMO systems can use either decode-and-forward (DF), amplify-and-forward (AF), or compress-and-forward (CF) protocol.

The EE performance of these relay protocols has been studied in [10]–[12], where a classical relay channel (with three single-antenna nodes) is considered. In [10] and [11], a linear approximation of the EE-SE trade-off is derived for relay communications by using the first and second derivatives of the channel capacity. This study is then extended in [12] where the synchronization between the transmitter and the relay is considered for practical scenarios. The approximation of the EE-SE trade-off in these previous papers is accurate in the low SE region but largely inaccurate otherwise. In addition, the aforementioned papers do not take circuit energy into consideration, which may not be negligible in practical wireless networks [8]. A more accurate approximation of the EE-SE trade-off for MIMO Rayleigh fading channels is presented in [6]: The approximation is in closed form, but the expression cannot be extended to a cooperative virtual-MIMO scheme. An initial study of virtual-MIMO based cooperative communications for distributed wireless sensor networks is given in [13], where the energy consumption of a traditional MIMO system and that of a virtual-MIMO scheme are evaluated. This work is then extended in [14] by taking into account the properties of the propagation environment and the energy overhead required for channel estimation. The corresponding energy consumption assessments of virtual-MIMO systems in [13] and [14] are based on numerical results and are applicable for the specific configurations considered in these papers.

An important open problem in virtual-MIMO communications is to obtain a general analytic formula for EE as a function of SE, and use it to identify the potential ways to improve EE. However, calculations of the system ergodic capacity in Rayleigh fading channels require taking expectations with respect to a random channel matrix. In general, the problem of defining an explicit expression to link EE and SE requires an expression for the inverse function of the capacity, and therefore is a mathematically challenging task. In this paper, we derive an accurate upper bound of EE as a function of SE for a virtual-MIMO system using receiver-side cooperation with the CF protocol. To get a full picture of the overall EE for the system, both transmit energy and circuit energy consumed at the transmitter and relay nodes are taken into account. A comparison between different relay protocols in terms of EE is also given in this paper. The main contributions of this paper are summarized as follows:

- We analyze the relationship between EE and SE for a virtual-MIMO system where a realistic power model is considered. To this end, we derive a tight closed-form upper bound for the ergodic capacity of the system, based on which we propose a novel upper bound for EE as a function of SE which exhibits a good accuracy for a wide range of SE values. The EE upper bound is used for assessing the EE ratios of virtual-MIMO over the ideal MIMO or the non-cooperative MISO system.
- We formulate an EE optimization problem based on the EE upper bound. Given a target SE, the optimal power allocation (between the transmitter and the relay) and optimal bandwidth allocation (between the data and cooperation channels) are derived such that the overall EE is maximized. The optimal solution for power allocation is obtained in a closed-form expression when an out-of-band cooperation channel is used.
- To capture the cost of cooperation, we place power constraints in the system, and investigate different bandwidth allocation scenarios for the data and cooperation channels. We show that the EE performance of virtual-MIMO is close to that of MIMO when an out-of-band cooperation channel is considered. Taking a shared-band cooperation channel into account, virtual-MIMO with equal bandwidth allocation is less energy efficient than MISO; but with optimal power and bandwidth allocation, virtual-MIMO outperforms MISO in terms of EE under most values of SE.

The rest of this paper is organized as follows. Section II describes the channel model and the realistic power model. Section III evaluates the relationship between EE and SE of virtual-MIMO, including deriving an accurate upper bound of EE in Section III-B. EE optimization issues are investigated in Section IV. Simulation results are in Section V, and Section VI concludes the paper.

II. System Model

We consider a transmitter node with N_t antennas and a destination node with a single antenna, as shown in Fig. 1. There are $N_r - 1$ single-antenna relays in the proximity of the destination. We refer to the destination and relays as the receiver group, which together with the transmitter form

a virtual-MIMO system [4]. We assume that the nodes within the receiver group are close, but the distance between the transmitter and the receiver group is large. For the sake of demonstrating performance of EE with more tractable mathematical expressions, we consider $N_t = N_r = 2$ in this paper. There are two orthogonal communication channels: the data channel between the transmitter and the receiver group, and the cooperation channel between the receivers.

A. Channel Model

In Fig. 1, $\boldsymbol{x} = [x_1, x_2]^{\mathrm{T}}$ denotes the transmitted signals, and $[y_r, y_d]^{\mathrm{T}}$ denotes the corresponding received signals at the relay and the destination. Without loss of generality, the data channels are represented by $h_i = \dfrac{c_i}{\sqrt{K_t} d^{\zeta/2}}$ $(i \in [1, ..., 4])$, where c_i is a circularly symmetric complex Gaussian random variable with unit variance and zero mean. As the relay is close to the destination, we assume that they are equally distanced from the transmitter, which is denoted by d. The scalar ζ is the path loss exponent, and K_t is a constant indicating the physical characteristics of the channel and the power amplifier [15]. That is, the data channels are modeled as Rayleigh fading with $\mathbb{E}[|h_i|^2] = 1/(K_t d^{\zeta})$. In matrix form, the received signal vector is

$$\begin{bmatrix} y_r \\ \\ y_d \end{bmatrix} = \boldsymbol{H}\boldsymbol{x} + \boldsymbol{n}; \quad \boldsymbol{H} = \begin{bmatrix} h_1 & h_2 \\ \\ h_3 & h_4 \end{bmatrix}, \tag{1}$$

where the data channel matrix $\boldsymbol{H} \in \mathbb{C}^{N_r \times N_t}$ is complex Gaussian distributed. $\boldsymbol{n} = [n_1, n_2]^{\mathrm{T}}$ is the noise vector with components $n_1, n_2 \sim \mathcal{CN}(0, N_0)$. We assume that perfect CSI is available at the receiver side only. Let W denote the bandwidth of the data channel. And suppose that the two antennas at the transmitter use the same average transmit power P_{st}, i.e., $\mathbb{E}[|x_1|^2] = \mathbb{E}[|x_2|^2] = P_{st}$. Here we consider equal power allocation among the transmit antennas as it is an optimal power allocation when no CSI is available at the transmitter side [16].

At the receiver group side, there is a short-range cooperation channel between the relay and the destination, which is modeled as an AWGN channel. The relative power gain of the cooperation channel to the power gain of data channels is represented by G. As the receivers are closer in our system model, the case of interest is when G is high. W_r and P_{rt} denote the bandwidth of

the cooperation channel and the transmit power of the relay, respectively.

B. Realistic Energy Consumption

In a practical setting, to quantify the total energy consumption of the entire system, both the transmit energy and circuit energy consumed at the transmitter and the relay need to be considered. For instance in [8] and [17], the total supply energy at a base station includes the energy consumed for the power amplifier, radio frequency circuitry, baseband unit, direct current (DC)-DC and alternating current (AC)-DC converters. In general, the total supply power and the transmit power at a base station is nearly linear and, consequently, a linear power model has been defined in [8] and adopted in this paper. Therefore at the transmitter, the total power for N_t antennas is given by $N_t(\xi_s P_{st} + P_{sc})$, where P_{sc} is the load-independent circuit power at the minimum nearly-zero output power, and ξ_s is the scaling factor of the load-dependent power. For the relay, using a similar linear power model, we have the total supply power $(\xi_r P_{rt} + P_{rc})$, where P_{rc} denotes the load-independent circuit power at the relay. Note that the scaling over signal load (i.e. the values of ξ_s and ξ_r) largely depends on the type of the station. Table 2 in [8] presents the model parameters for various transmitter types in a 3GPP LTE network, and Table I in [18] presents the parameters for the relay model, which could be adopted in our system.

We assume that the transmitter and the relay are subject to separate power constraints: $0 < P_{st} \leq P_{\text{max,s}}$ and $0 < P_{rt} \leq P_{\text{max,r}}$. For the relay, we define $\gamma = P_{rt}/P_{st}$ to be the power allocation ratio between the relay and the transmitter. Compared to a total power constraint, this assumption of separate power constraints is more practical for wireless networks, because the transmitter and relay are usually geographically separated and are supported by separate power supplies [19]. With the knowledge of P_{st}, the relay will decide its own transmit power (via choosing a value of γ). Finally, the total power of the entire system is

$$\begin{aligned} &P_{\text{tot}} = N_t(\xi_s P_{st} + P_{sc}) + \xi_r P_{rt} + P_{rc} = (N_t\xi_s + \gamma\xi_r)P_{st} + N_t P_{sc} + P_{rc}; \\ &0 < P_{st} \leq P_{\text{max,s}},\ 0 < \gamma \leq P_{\text{max,r}}/P_{st}. \end{aligned} \tag{2}$$

C. Impact of Relay Protocol

Relay protocols are usually classified into three categories: DF, AF, and CF, which require different signal processing techniques at the relay. But these techniques have a similar complexity. Since the power consumed in the baseband unit is mainly defined by the complexity, the power difference of the three protocols (caused by different signal processing techniques) is quite small compared with other parts of the circuit power (such as that for the radio frequency circuitry), and can be neglected. We thus consider the circuit power at the relay P_{rc} remains the same for the three relay protocols. In addition, the relay is assumed to be closer to the destination in this paper; compared to DF, the CF protocol provides superior capacity performance [5], [20]. Therefore, given the same P_{rt}, DF and CF have the same total power consumption; but CF is more spectrally efficient. According to the definition of EE, CF has a better EE than DF.

In addition, the AF protocol is a special case of CF, in which case the relay simply scales and forwards the analog signal waveform that is received from the transmitter without any particular processing [21]. AF requires equal bandwidth allocation for the data and cooperation channels, as the amplified analog signal needs to occupy an unchanged bandwidth. But, for CF, the signal at the relay is quantized and can be re-encoded, so that the bandwidth of the cooperation channel can be changed and optimized as will be shown in Section IV-B. Therefore, for any given channel conditions, CF performs better than or equal to AF in terms of their EE performance. Thus in this paper, we assume the relay sends its observation to the destination implementing CF cooperation, where a standard source coding technique [5] is used by the relay.

III. Spectral Efficiency and Energy Efficiency of the Virtual-MIMO System

In this section, we evaluate the relationship between EE and SE of the virtual-MIMO system. We first obtain a tight closed-form upper bound for the ergodic capacity of the system. Then an explicit and accurate approximation of the EE as a function of SE is derived, and is utilized for assessing analytically the EE gain or loss of virtual-MIMO over the MISO or MIMO systems.

A. Ergodic Capacity of Virtual-MIMO: Explicit Expression VS. Upper Bound

The system model that specified in Section II can be considered as a system where the destination has two antennas that receive the signals $[y_r + n_c, y_d]^{\mathrm{T}}$ [20]. Here $n_c \sim \mathcal{CN}(0, \sigma_c^2)$ is the compression noise, which results from the CF protocol. As we employ a standard source coding technique to implement the CF protocol at the relay, we denote R_c as the source coding rate at the relay which is (smaller than but arbitrarily close to) [2], [22]

$$R_c = W_r \log_2 \left(1 + \frac{G}{K_t d^{\zeta}} \cdot \frac{P_{rt}}{N_0 W_r}\right). \tag{3}$$

Then the variance of the compression noise n_c is [2]

$$\sigma_c^2 = \frac{\mathbb{E}[|y_r|^2]}{2^{R_c/W} - 1} = \frac{(|h_1|^2 + |h_2|^2)P_{st} + N_0 W}{\left[1 + \frac{G}{K_t d^{\zeta}} \cdot \frac{P_{rt}}{N_0 W_r}\right]^{W_r/W} - 1}. \tag{4}$$

The value of σ_c^2 is related to R_c, and thus determined by channel conditions and energy consumption. The destination scales $y_r + n_c$ using the degradation factor η, such that $\sqrt{\eta}(y_r + n_c)$ and y_d have the same power of additive Gaussian noise [5]; thus

$$\tilde{\boldsymbol{y}} = [\sqrt{\eta}(y_r + n_c), y_d]^{\mathrm{T}} = \widetilde{\boldsymbol{H}}\boldsymbol{x} + [\tilde{n}_1, n_2]^{\mathrm{T}}; \quad \widetilde{\boldsymbol{H}} \triangleq \begin{bmatrix} \sqrt{\eta}h_1 & \sqrt{\eta}h_2 \\ h_3 & h_4 \end{bmatrix}; \quad \eta \triangleq \frac{N_0 W}{N_0 W + \sigma_c^2}, \tag{5}$$

where $\tilde{n}_1 \sim$ i.i.d. $\mathcal{CN}(0, N_0)$. In (4), if $|h_1|^2 + |h_2|^2$ could be replaced by its expected value, η in (5) would become constant given certain average channel condition and energy consumption, and therefore the scaled channel $\widetilde{\boldsymbol{H}}$ would be a complex Gaussian matrix. The numerical results in [4] have demonstrated the accuracy of this replacement. Thus it is reasonably appropriate to implement the expectation of η (denoted by $\bar{\eta}$) for the distribution analysis of $\widetilde{\boldsymbol{H}}$ and the corresponding capacity evaluation. Then from (4) and (5), we have

$$\bar{\eta} = \frac{\left[1 + \frac{G}{K_t d^{\zeta}} \cdot \frac{\gamma P_{st}}{N_0 W_r}\right]^{W_r/W} - 1}{\left[1 + \frac{G}{K_t d^{\zeta}} \cdot \frac{\gamma P_{st}}{N_0 W_r}\right]^{W_r/W} + \frac{2P_{st}}{(K_t d^{\zeta} N_0 W)}}, \tag{6}$$

and $\widetilde{\boldsymbol{H}} \sim \mathcal{CN}_{N_r,N_t}(0,\, \boldsymbol{\Psi} \otimes \boldsymbol{I})$. $\boldsymbol{\Psi}$ is the covariance matrix

$$\boldsymbol{\Psi} = \mathbb{E}\left[\begin{pmatrix} \sqrt{\bar{\eta}} h_1 \\ h_3 \end{pmatrix} \begin{pmatrix} \sqrt{\bar{\eta}} h_1 & h_3 \end{pmatrix}\right] = \begin{bmatrix} \bar{\eta}/(K_t d^{\zeta}) & 0 \\ 0 & 1/(K_t d^{\zeta}) \end{bmatrix}. \tag{7}$$

Then $\boldsymbol{\Xi} = \widetilde{\boldsymbol{H}}\widetilde{\boldsymbol{H}}^{\dagger}$ has a complex central Wishart distribution with N_t degrees of freedom and covariance matrix $\boldsymbol{\Psi}$, i.e. $\boldsymbol{\Xi} \sim \mathcal{CW}_{N_r}(N_t, \boldsymbol{\Psi})$. Here $N_t \geq N_r$ is considered. In the following lemma, we give a result on the complex central Wishart matrix.

Lemma 1: If $\boldsymbol{Y} \sim \mathcal{CW}_{N_r}(N_t, \boldsymbol{\Psi})$, then we have

$$\mathbb{E}[\det(\boldsymbol{Y})] = \det(\boldsymbol{\Psi}) \prod_{j=0}^{N_r-1} (N_t - j). \tag{8}$$

The proof of Lemma 1 is given in Appendix A.

With the CF protocol, the ergodic capacity of the virtual-MIMO system is given by [5], [22]

$$C_{\text{CF}} = \mathbb{E}\left[W \log_2 \det\left(\boldsymbol{I} + \frac{P_{st}}{N_0 W}\boldsymbol{\Xi}\right)\right] \quad \text{bits/s}. \tag{9}$$

The following result gives a upper bound for the explicit expression of ergodic capacity when signal-to-noise ratio (SNR) is not low.

Proposition 1: If $\widetilde{\boldsymbol{H}} \sim \mathcal{CN}_{N_r,N_t}(0,\, \boldsymbol{\Psi} \otimes \boldsymbol{I})$, i.e. for the considered virtual-MIMO system with CF cooperation, when SNR is not low, the ergodic capacity upper bound $\widehat{C}_{\text{CF}}$ is

$$\widehat{C}_{\text{CF}} = W\left[N_r \log_2\left(\frac{P_{st}}{N_0 W}\right) + \log_2\left[\frac{N_t!}{(N_t - N_r)!}\right] + \log_2 \det(\boldsymbol{\Psi})\right] \quad \text{bits/s}. \tag{10}$$

The proof of Proposition 1 is given in Appendix B. This proposition provides a simple and tight upper bound of the ergodic capacity, which is less accurate than the explicit expression (9), but has the advantage of being express in a closed form and can be used to evaluate the relationship between EE and SE for the virtual-MIMO system.

B. Upper Bound on Energy Efficiency

We use the well known definition of the system achievable EE as the number of bits transmitted per Joule of energy, i.e. $E_{\text{CF}} = C_{\text{CF}}/P_{\text{tot}}$ in bits/Joule. According to equations (2) and (9), both P_{tot} and C_{CF} are related to the transmit power P_{st}. Thus the impact of C_{CF} on E_{CF} can be expressed as follows

$$E_{\text{CF}} = C_{\text{CF}} \left[(N_t \xi_s + \gamma \xi_r) f^{-1}(C_{\text{CF}}) + N_t P_{sc} + P_{rc} \right]^{-1}, \tag{11}$$

where f^{-1}: $C_{\text{CF}} \mapsto P_{st}$ is the inverse function of C_{CF}. Equation (11) indicates that obtaining an explicit expression of E_{CF} boils down to finding an explicit formula for $f^{-1}(C_{\text{CF}})$. However, due to the random Rayleigh channel realizations, $f^{-1}(C_{\text{CF}})$ does not have a straightforward formulation. One feasible approach would be to use the closed-form upper bound of C_{CF} in (10) for finding an explicit solution to $f^{-1}(C_{\text{CF}})$. This approach will help us obtain a EE upper bound as a function of SE, which can be used for explicitly tracking the EE performance and analytically assessing the EE optimizations for a given SE, and thus will be discussed in this subsection.

We use S_{CF} to denote SE of the system. Two scenarios of the bandwidth allocation between the data channel and the cooperation channel are considered in this paper: Scenario I, the relay uses out-of-band channel for cooperation; Scenario II, the relay uses a portion of the whole channel. In Scenario I, we assume the data channel and the out-of-band cooperation channel have equal bandwidth, i.e. $W_r = W$. As suggested in [2], this is applicable when the separate band used for short-range cooperation can be spatially reused across all other cooperating nodes in a network and hence the bandwidth cost for a particular cooperating pair can be neglected here. In Scenario II, a single channel is divided into two different bands to implement the cooperation. Scenario II is applicable when spatial reuse of cooperation bands is not considered, i.e., the cooperation channel needs to share the band used for data transmission. To account for the bandwidth allocation, we define $\phi = W_r/W$. Therefore, we have $S_{\text{CF}}(E_{\text{CF}}) = \frac{C_{\text{CF}}(P_{st})}{W}$ for bandwidth Scenario I, and $S_{\text{CF}}(E_{\text{CF}}) = \frac{C_{\text{CF}}(P_{st})}{W+W_r}$ for bandwidth Scenario II. The choice of S_{CF}

and C_{CF} differentiates SE and system capacity, and also helps avoid the abuse of notations that correspond to the functions of E_{CF} and P_{st} [12].

1) Bandwidth Scenario I:

For Scenario I, when W=W_r, (6) is further simplified

$$\bar{\eta} = \frac{G\gamma P_{st}}{K_t d^{\zeta} N_0 W + G\gamma P_{st} + 2P_{st}}. \tag{12}$$

Inserting (12) in (7), and from (10), we have

$$\widehat{C}_{\text{CF}} = W\left[2\log_2\left(\frac{P_{st}}{K_t d^{\zeta}\, N_0 W}\right) + 1 + \log_2\left(\frac{G\gamma P_{st}}{K_t d^{\zeta} N_0 W + G\gamma P_{st} + 2P_{st}}\right)\right] \quad \text{bits/s.} \tag{13}$$

According to the definition of EE, we can obtain a closed-form upper bound for the system EE as shown in the following.

Proposition 2: Consider the virtual-MIMO system with CF cooperation. For Scenario I, the upper bound for the number of bits transmitted per Joule of energy, denoted by $\widehat{E}_{\text{CF}}$, is

$$\widehat{E}_{\text{CF}} = W S_{\text{CF}}\left[(2\xi_s + \gamma\xi_r)2^{\frac{S_{\text{CF}}}{2}-\frac{1}{2}} K_t d^{\zeta} N_0 W\sqrt{\frac{G\gamma+2}{G\gamma}} + 2P_{sc} + P_{rc}\right]^{-1},$$
$$\text{with}\ \ S_{\text{CF}} \le 2\log_2\left[P_{\text{max,s}}/(K_t d^{\zeta}\, N_0 W)\right] + 1 + \log_2\left[G\gamma/(G\gamma+2)\right]. \tag{14}$$

The proof of Proposition 2 is given in Appendix C.

For Scenario I, the EE upper bound $\widehat{E}_{\text{CF}}$ is obtained in closed form, and thus the relationship between EE and SE is explicit. The closed-form EE upper bound and its application environment (i.e. Scenario I) are particularly valuable and attractive to some realistic wireless communication systems. For example, the closely located relay and destination could perform cooperation through their out-of-band Wi-Fi without sharing the frequency bands for data channel that uses 3G (or 4G) cellular communications.

In addition, as shown in (14), P_{sc} and P_{rc} are the load-independent circuit power at the transmitter and the relay, and therefore remain the same for various S_{CF}. When S_{CF} is small, P_{sc} and P_{rc} dominate the EE performance, and thus E_{CF} is very low. With S_{CF} increasing, E_{CF} increases but will finally decrease. Therefore, compared to the case without considering circuit

energy consumption, there is no longer a monotonic trade-off relationship between EE and SE for this system. There exists a certain region of SE that corresponds to a better EE performance, as will shown in Section V.

2) Bandwidth Scenario II:

We now consider a single channel to be divided into two different bands to implement the cooperation, and demonstrate its impact on the EE analysis. Using $\phi = W_r/W$, (6) is shown as

$$\bar{\eta} = \frac{\left(N_0 W K_t d^{\zeta} + G\gamma P_{st}/\phi\right)^{\phi} - N_0 W K_t d^{\zeta}}{\left(N_0 W K_t d^{\zeta} + G\gamma P_{st}/\phi\right)^{\phi} + 2P_{st}}. \tag{15}$$

Inserting (15) in (7), and from (10), we have

$$\widehat{C}_{\text{CF}} = W\left[2\log_2\left(\frac{P_{st}}{K_t d^{\zeta} N_0 W}\right) + 1 + \log_2\left(\frac{\left(N_0 W K_t d^{\zeta} + G\gamma P_{st}/\phi\right)^{\phi} - N_0 W K_t d^{\zeta}}{\left(N_0 W K_t d^{\zeta} + G\gamma P_{st}/\phi\right)^{\phi} + 2P_{st}}\right)\right]. \tag{16}$$

Different from (13), we cannot get a closed-form solution for P_{st} from (16) because of ϕ. To give an explicit relationship between EE and SE under this scenario, we represent the solution of (16) as follows

$$P_{st} = f^{-1}(\widehat{C}_{\text{CF}}) = K_t d^{\zeta} N_0 W \cdot \mathcal{R}_P\left\{2^{S_{\text{CF}}(1+\phi)} - 2P^2\frac{(1+G\gamma P/\phi)^{\phi} - 1}{(1+G\gamma P/\phi)^{\phi} + 2P}\right\}, \tag{17}$$

where $P = P_{st}/(N_0 W K_t d^{\zeta})$, and the function $\mathcal{R}_P\{g(P)\}$ denotes the exact roots of the equation $g(P) = 0$ with respect to its single variable P. Note that one can apply differentiation or partial differentiation to $\mathcal{R}_P\{g(P)\}$. Substituting (17) into (11), and let $S_{\text{CF}} = \frac{C_{\text{CF}}}{(1+\phi)W}$, we thus obtain a EE upper bound for Scenario II as shown in the following.

Proposition 3: Consider the virtual-MIMO system with CF cooperation. For Scenario II, the upper bound for the amount of bits transmitted per Joule of energy can be represented as

$$\widehat{E}_{\text{CF}} = \frac{S_{\text{CF}}/(K_t d^{\zeta} N_0)}{\frac{2P_{sc}+P_{rc}}{K_t d^{\zeta} N_0 W} + (2\xi_s + \gamma\xi_r)\cdot\mathcal{R}_P\left\{2^{S_{\text{CF}}(1+\phi)} - 2P^2\frac{(1+G\gamma P/\phi)^{\phi}-1}{(1+G\gamma P/\phi)^{\phi}+2P}\right\}}. \tag{18}$$

Here S_{CF} is also restricted by $P_{\text{max,s}}$; Replacing P_{st} by $P_{\text{max,s}}$ in (16) gives the constraint on S_{CF}.

Given some values of ϕ, the roots $\mathcal{R}_P\{g(P)\}$ can be represented in closed form. Taking $\phi = 1$

for example, i.e. $W_r = W$, we have

$$\mathcal{R}_P\left\{2^{S_{\text{CF}}(1+\phi)}-2P^2\frac{(1+G\gamma P/\phi)^{\phi}-1}{(1+G\gamma P/\phi)^{\phi}+2P}\right\}\approx\mathcal{R}_P\left\{2^{2S_{\text{CF}}}-\frac{2P^2G\gamma}{G\gamma+2}\right\}=2^{S_{\text{CF}}}\sqrt{\frac{G\gamma+2}{2G\gamma}}. \quad (19)$$

Inserting (19) to (18), the closed-form EE upper bound for Scenario II is obtained. For some other values of ϕ, if the roots cannot be represented in a simple form, one can use Newton's method to find approximations to the roots. The EE upper bound in Proposition 3 removes the effects of random channel variations, and thus can be used for explicitly tracking the EE performance of virtual-MIMO, and analytically assessing the EE gain or loss of virtual-MIMO over the MISO or MIMO system.

3) On Energy Efficiency Comparisons:

The EE upper bound of the ideal MIMO system (as if the receivers were connected via a wire) and that of the non-cooperative MISO system (where the relay is silent) are given by

$$\widehat{E}_{\text{MIMO}}=\frac{WS_{\text{MIMO}}}{2P_{sc}+\xi_s 2^{\frac{S_{\text{MIMO}}-1}{2}}K_t d^{\zeta}N_0W}, \text{ where } S_{\text{MIMO}}\leq 2\log_2\left[P_{\text{max,s}}/(K_t d^{\zeta}N_0W)\right]+1; \quad (20)$$

$$\widehat{E}_{\text{MISO}}=\frac{WS_{\text{MISO}}}{2P_{sc}+\xi_s\left(2^{S_{\text{MISO}}}-1\right)K_t d^{\zeta}N_0W}, \text{ where } S_{\text{MISO}}\leq\log_2\left[1+P_{\text{max,s}}/(K_t d^{\zeta}N_0W)\right]. \quad (21)$$

To obtain (20), we solve P_{st} from (10) where the covariance matrix $\boldsymbol{\Psi}=\boldsymbol{I}$ for the ideal MIMO case. Then substituting the solution of P_{st} into the EE expression $E_{\text{MIMO}}=\frac{WS_{\text{MIMO}}}{N_t(P_{sc}+\xi_s P_{st})}$, and considering the power constraint $0<P_{st}\leq P_{\text{max,s}}$, we thus obtain (20). In a similar way, but taking into account $N_t=2$ and $N_r=1$, we get (21) for the MISO case.

In order to evaluate how virtual-MIMO compared with MIMO and MISO systems in terms of EE, we use the EE ratios $E_{\text{MIMO}}/E_{\text{CF}}$ and $E_{\text{MISO}}/E_{\text{CF}}$. For a certain value of SE, the EE ratios boil down to the total power ratios of the corresponding systems. We first consider bandwidth Scenario I for the virtual-MIMO system. The theoretical EE ratios of MIMO over virtual-MIMO in the low and high-SE regimes, respectively, can be approximated as

$$\lim_{SE\to 0}\frac{E_{\text{MIMO}}}{E_{\text{CF}}}=\frac{2P_{sc}+P_{rc}}{2P_{sc}}; \qquad \lim_{SE\to\infty}\frac{E_{\text{MIMO}}}{E_{\text{CF}}}\approx\lim_{SE\to\infty}\frac{\widehat{E}_{\text{MIMO}}}{\widehat{E}_{\text{CF}}}=\sqrt{\frac{G\gamma+2}{G\gamma}}\cdot\frac{2\xi_s+\gamma\xi_r}{2\xi_s}. \quad (22)$$

In the low SE regime, the load-independent circuit power dominates the EE ratios. With SE increasing (when no SE constraint is considered), the ratio of $E_{\text{MIMO}}/E_{\text{CF}}$ finally approaches a constant value, as will be illustrated in Section V. Similarly, the theoretical EE ratios of MISO over virtual-MIMO are given by

$$\lim_{SE\to 0}\frac{E_{\text{MISO}}}{E_{\text{CF}}}=\frac{2P_{sc}+P_{rc}}{2P_{sc}};\qquad \lim_{SE\to\infty}\frac{E_{\text{MISO}}}{E_{\text{CF}}}\approx\lim_{SE\to\infty}\frac{\widehat{E}_{\text{MISO}}}{\widehat{E}_{\text{CF}}}=0. \tag{23}$$

Because of the additional P_{rc}, virtual-MIMO has a slight EE performance loss compared to the MISO case in the low SE regime. But when SE is high, virtual-MIMO performs much better than MISO as the ratio $E_{\text{MISO}}/E_{\text{CF}}$ approaches zero.

For virtual-MIMO with Scenario II, we consider a special case: equal bandwidth is allocated for the data and cooperation channels, i.e. $\phi=1$. Inserting (19) to (18), we obtain $\widehat{E}_{\text{CF},\phi=1}$ for this case, and then have the EE ratios as follows

$$\lim_{SE\to 0}\frac{E_{\text{MISO}}}{E_{\text{CF},\phi=1}}=\frac{2P_{sc}+P_{rc}}{2P_{sc}};\qquad \lim_{SE\to\infty}\frac{E_{\text{MISO}}}{E_{\text{CF},\phi=1}}\approx\lim_{SE\to\infty}\frac{\widehat{E}_{\text{MISO}}}{\widehat{E}_{\text{CF},\phi=1}}=\frac{2\xi_s+\gamma\xi_r}{\sqrt{2}\xi_s}\sqrt{\frac{G\gamma+2}{G\gamma}}. \tag{24}$$

As shown in (24), $\lim_{SE\to\infty}\dfrac{E_{\text{MISO}}}{E_{\text{CF},\phi=1}}\geq 1$, which means even in the high-SE regime, equal bandwidth allocation results in the virtual-MIMO performing worse than the MISO case. An optimal bandwidth allocation for Scenario II to maximize EE of virtual-MIMO is thus a non-trivial problem and will be discussed in this following section.

IV. Energy Efficiency Optimizations

In this section, we consider EE optimization issues for the virtual-MIMO system under both the bandwidth Scenario I and Scenario II. The optimization criterion is based on the tight upper bound of EE. The impact of different relay protocols on EE is also studied. Finally we generalize the EE performance for a virtual-MIMO system with more antennas and more cooperating nodes.

A. Optimal Power Allocation

To investigate the EE performance of the virtual-MIMO system, we aim to obtain the maximum E_{CF} for a certain level of SE. The explicit expression of EE upper bound $\widehat{E}_{\text{CF}}$ for Scenario I in

(14) shows that for a specific capacity-achieving transmission rate and given channel conditions, different values of γ represent different levels of EE, power allocation between the transmitter and the relay is an efficient way to improve EE. Based on the closed-form EE upper bound, we formulate the EE optimization problem for Scenario I as follows

$$\max_{\gamma} \widehat{E}_{\text{CF}}(\gamma), \quad \text{subject to } 0 < \gamma \leq P_{\text{max,r}}/P_{st}. \tag{25}$$

We aim to choose a value of γ such that the upper bound of E_{CF} for a specific transmission rate is maximized.

One can apply a concave optimization algorithm to find the optimal solution for (25). The proof that $\widehat{E}_{\text{CF}}(\gamma)$ is a concave function with respect to $\gamma \in (0, P_{\text{max,r}}/P_{st}]$ can be found in Appendix D. Thus, the local extremum of $\widehat{E}_{\text{CF}}(\gamma)$ is also a global extremum. We use Fermat's theorem to find the local extremum: By setting $\frac{\partial P_{\text{tot}}(\gamma)}{\partial \gamma} = 0$ in (35), one can obtain an unique closed-form solution γ^*

$$\gamma^* = \min\left\{ \frac{-\xi_r + \sqrt{\xi_r^2 + 8\xi_r G \xi_s}}{2\xi_r G}, \sqrt{\frac{P_{\text{max,r}}^2}{2^{S_{\text{CF}}-1}(K_t d^{\zeta} N_0 W)^2} + \frac{1}{G^2}} - \frac{1}{G} \right\}. \tag{26}$$

The solution γ^* represents the optimal power allocation between the transmitter and the relay, which is independent of the data channel conditions and the values of SE. This closed-form solution makes the EE optimization easy to implement in practice: For specific power scaling factors ξ_s and ξ_r, the relay can dynamically change its transmit power level (by using $P_{rt} = \gamma^* P_{st}$) according to the expected value of G, such that the virtual-MIMO EE performance will be maximized.

B. Joint Power and Bandwidth Allocation

In Scenario I, ϕ is fixed at 1 and spatial reuse of the cooperation bandwidth is considered. When such spatial reuse is not applicable, i.e. under Scenario II, bandwidth allocation needs to be performed and thus, ϕ is optimized jointly with power allocation to maximize the system EE.

Based on the upper bound of $\widehat{E}_{\text{CF}}$ in (18), we formulate the EE optimization problem as

follows

$$\max_{\gamma,\phi\in\mathbb{R}^+} : \widehat{E}_{\text{CF}}(\gamma,\phi), \quad \text{subject to } \gamma - P_{\text{max,r}}/P_{st} \leq 0 \text{ and } \phi - 1 \leq 0 \ . \tag{27}$$

Different from (25), there exist two constraints where joint power and bandwidth allocation is considered. The solution of the above optimization problem is not straightforward. One can apply the method of Lagrange multiplier to find the solution. The proof that $\widehat{E}_{\text{CF}}(\gamma,\phi)$ is a concave function with respect to $\gamma \in (0, P_{\text{max,r}}/P_{st}]$ and $\phi \in (0,1]$ can be found in Appendix E.

We convert the primal problem (i.e. the original form of the optimization problem in (27)) to a dual form. The corresponding Lagrangian function is defined as

$$L(\gamma,\phi,\rho,\mu) \stackrel{\triangle}{=} E_{\text{CF}}(\gamma,\phi) - \rho(\gamma - P_{\text{max,r}}/P_{st}) - \mu(\phi - 1), \tag{28}$$

where ρ and μ are Lagrangian multipliers. Thus, solving the primal problem of (25) is equivalent to solving its dual problem $\min\limits_{\rho,\mu} \max\limits_{\gamma,\phi\in\mathbb{R}^+} L(\gamma,\phi,\rho,\mu)$.

The optimization algorithm is summarized in Table I: We adopt the subgradient method to solve the dual problem. As shown in step (b), where $[x]^+ = \max(0,x)$, $\tau_1^{(k)}$ and $\tau_2^{(k)}$ denote the step sizes which are small positive parameters, and $g_1^{(k)} = P_{\text{max,r}}/P_{st} - \gamma^{(k)}$ and $g_2^{(k)} = 1 - \phi^{(k)}$ are subgradients. We denote $\gamma^\dagger(\rho^{(k)},\mu^{(k)})$ and $\phi^\dagger(\rho^{(k)},\mu^{(k)})$ as the solutions of the two subproblems [23]: Subproblem 1, $\max_{\gamma\in\mathbb{R}^+} L(\gamma)$, and Subproblem 2, $\max_{\phi\in\mathbb{R}^+} L(\phi)$, respectively. We use the Karush-Kuhn-Tucker (KKT) conditions for solving the above subproblems [24]. That is, we obtain $\gamma^\dagger(\rho^{(k)},\mu^{(k)})$ and $\phi^\dagger(\rho^{(k)},\mu^{(k)})$ from step (a) in Table I, The subgradient algorithm is then applied to update the parameters. Repeating these steps until Lagrangian function converges, we thus get the solutions of the optimization problem. The final optimal values of $\gamma^\dagger$ and $\phi^\dagger$ represent the optimal power and bandwidth allocation that help maximize EE of the system.

V. Simulation Results and Discussions

In this section, we present the EE performance and the influence of SE on EE for the virtual-MIMO system by using both simulation and analytical results. The simulation results are obtained from the Monte Carlo method for random channel realizations. The major simulation parameters

are listed in Table II unless otherwise stated. The physical channel propagation parameters are adopted from the 3GPP LTE standard models [9], [17]. The values of the power model parameters for the transmitter are suggested by [8] where a Macro type of transmitter is considered. A potential introduction of relay nodes for LTE-Advanced is to be included in Release 10 and is expected not before 2014. Thus, here we adopt an estimation of the relay power model as suggested by [18].

A. EE and Its Relationship with SE

Firstly, we verify the validity and accuracy of the SE upper bound given by Proposition 1 for the Virtual-MIMO system and that considering $\boldsymbol{\Psi} = \boldsymbol{I}$ for the $N_t \times N_r$ MIMO case in Fig. 2. For virtual-MIMO, we consider $G = 10$ dB and $\gamma = 0.25$, where the value of G is selected because of the assumption of short-range cooperation channel. The transmit power of the relay is smaller than that of the transmitter which justifies the chosen value for γ. We consider bandwidth Scenario I for the virtual-MIMO using CF protocol. This figure shows that the virtual-MIMO with CF under Scenario I has a SE performance very close to the MIMO system. We can also see that the upper bounds are quite tight for the entire range of P_{st}, regardless of the number of antennas, no matter for MIMO or Virtual-MIMO. The tightness of the SE upper bounds is very important to guarantee the accuracy of EE upper bounds.

Using the above settings of G and γ, we analyze EE of the virtual-MIMO system with CF for Scenario I and demonstrate the accuracy of the EE upper bound given by Proposition 2 in Fig. 3. As we consider transmit power constraints, the range of SE is limited as shown in this figure, where the edge of SE for virtual-MIMO is given by (14) and that for MIMO and MISO are given by (20) and (21), respectively. Fig. 3 (a) shows that the EE upper bounds are very tight to the simulation results for the whole range of SE, which is important for the optimization purposes. Fig. 3 (b) shows how the EE of virtual-MIMO compare to those of the MIMO and MISO systems by using EE ratios. In the low SE regime, both the ratios $E_{\text{MIMO}}/E_{\text{CF}}$ and $E_{\text{MISO}}/E_{\text{CF}}$ starts from a value slightly larger than 1, which corresponds to the results obtained from (22) and (23). With SE increasing, virtual-MIMO demonstrates a much better EE performance than

the non-cooperative MISO system, and performs close to the ideal MIMO case in terms of EE. Virtual-MIMO is thus particularly valuable to realistic wireless communications: With help from the relay, Virtual-MIMO enables base stations to become more energy efficient, and allows user devices to reap longer battery life.

Using the EE upper bounds given by Proposition 2, Fig. 4 shows how load-independent circuit power and load-dependent power components have meaningful impacts on the overall EE for both MISO/MIMO and virtual-MIMO with CF. The settings of G and γ remain the same as above. Fig. 4 (a) shows a trade-off relationship between EE and SE when only load-dependent power (i.e. $N_t\xi_s P_{st}$) is considered. The EE performance with total power is a combination of the effects from both load-independent circuit power (i.e. $N_t P_{sc}$) and load-dependent power. That is, when SE is low, EE is dominated by $N_t P_{sc}$. With SE increasing, the transmit power contributes more to P_{tot}; thus, EE increases up to a certain level but finally decreases. A similar trend can be seen in Fig. 4 (b) for virtual-MIMO, but the load-dependent power is $(N_t\xi_s + \gamma)P_{st}$ and the circuit power is $(N_t P_{sc} + P_{rc})$. Fig. 4 (b) also shows the impact of varying the distance from the transmitter to the receiver group on EE. A shorter distance (i.e. a smaller value of d) guarantees a higher EE and vice versa.

Our next analysis demonstrates the impact of different power allocation choices, defined by different values of γ, on EE of virtual-MIMO with CF for Scenario I. We choose specific capacity-achieving transmission rates, e.g., $S_{\text{CF}} = 10, 12$ bits/s/Hz, and consider $G = 10, 20$ dB. The results from this scenario are shown in Fig. 5. It is shown that different values of γ result in different levels of EE. The upper bound is very tight to the simulated EE, regardless the values of γ, and can therefore be used to predict the practical EE. Thus it is appropriate to implement the optimal $\gamma*$ which is computed from (26) to maximize the overall EE. As illustrated in this figure and shown in (26), taking the assumption $G = 10$ dB as an example, the optimal $\gamma*$ equals 0.53 for both $S_{\text{CF}} = 10$ and 12 bits/s/Hz.

B. EE Optimizations

We now demonstrate the optimal EE performance of virtual-MIMO with CF in this subsection, where optimal power allocation is performed for Scenario I and optimal joint power and bandwidth allocation is performed for Scenario II. Specifically, under Scenario I, with the optimal choices of $\gamma*$ computed from (26), the EE comparisons between virtual-MIMO and MIMO (for specific $S_{\text{CF}} = 8, 12$ bits/s/Hz) against the cooperation channel power gain G are shown in Fig. 6. As the results show, when G is small, EE of virtual-MIMO is impaired by energy consumption at the relay and also unstable transmission over the weak cooperation channel. As G increases, the helping relay enables virtual-MIMO to achieve a better EE performance very close to that of the ideal MIMO case. In addition, with a smaller value of S_{CF}, the EE performance is less affected by the conditions of the cooperation channel, as the load-independent circuit power is a dominant factor here.

We now extend the EE performance analysis to Scenario II, where bandwidth allocation needs to be optimized jointly with power allocation to maximize EE. $G = 20$ dB is considered in Fig. 7. We can see that the EE performance of virtual-MIMO with CF is much better than that of the MISO case, even though their performance gap is much smaller compared to Scenario I. In addition, to illustrate the benefit of CF cooperation for virtual-MIMO, we also show the results using AF in Fig. 7. As discussed in Section II-C, AF is a special case of CF where half of the total network bandwidth is allocated for cooperation. As the results demonstrate, CF with equal bandwidth allocation (i.e., the AF case) is even less energy efficient than MISO; but using the optimal power and bandwidth allocation, virtual-MIMO with CF outperforms MISO in terms of EE under most SE values.

In Fig. 8, EE comparisons among virtual-MIMO, ideal MIMO, and MISO as a function of G, are presented for different values of SE under Scenario II. Compared to the performance for Scenario I, a bigger loss exists for virtual-MIMO with CF against MIMO due to the extra cost for the cooperation bandwidth. Nevertheless, for both scenarios, similar impacts from the values of G on the EE performance are shown: When SE is low, EE of virtual-MIMO with CF is less affected by the conditions of the cooperation channel; When SE is high, a larger

value of G guarantees a better cooperation channel and thus results in higher EE performance of virtual-MIMO.

VI. Conclusion

This paper investigates EE performance of a virtual-MIMO system using receiver-side CF cooperation, where a realistic power model is considered. To account for the cost of cooperation, the allocation of power as well as bandwidth in the system are studied. We derive a tight closed-form upper bound for the ergodic capacity of the system, and based on which we propose a novel and accurate upper bound for EE as a function of SE. The EE upper bound is obtained in a closed-form expression when an out-of-band channel is used for cooperation. The EE upper bound exhibits a good accuracy for a wide range of SE values, and thus is utilized for explicitly tracking the EE performance of virtual-MIMO and analytically assessing the EE ratios of virtual-MIMO over the MIMO or MISO system.

Based on EE upper bound, we have formulated the EE optimization problem and demonstrated that for the virtual-MIMO system there exist two ways to improve EE: power allocation between the transmitter and the relay, and bandwidth allocation between the data and cooperation channels. Given a target SE, the system EE is maximized by using optimal power and bandwidth allocation, which provides much insight for designing practical virtual-MIMO systems. Results indicate that EE performance of virtual-MIMO is sensitive to many factors including resource allocation schemes and channel characteristics. In addition, EE performance of virtual-MIMO is close to MIMO when the out-of-band cooperation channel is considered. For the shared-band cooperation channel, virtual-MIMO with equal bandwidth allocation is less energy efficient than MISO; but with optimal power and bandwidth allocation, virtual-MIMO outperforms MISO in terms of EE under most values of SE. Virtual-MIMO is thus particularly valuable to realistic wireless communications: With the proposed scheme, Virtual-MIMO enables base stations to become more energy efficient, and allows user devices to reap longer battery life.

This paper focuses on the 2×2 virtual-MIMO system, i.e. two-antenna transmitter sending information to two single-antenna receivers. For the virtual-MIMO configuration with more

transmit antennas and more cooperating terminals, EE improvements over MISO can be expected only when the capacity improvement (because of cooperation) can compensate for the extra power required at the relays. Extending the analysis to more cooperating terminals, and studying suitable resource allocation schemes among the relays to guarantee EE benefits are left as future work.

APPENDIX A
PROOF OF LEMMA 1

If $\boldsymbol{Y} \sim \mathcal{CW}_{N_r}(N_t, \boldsymbol{\Psi})$, the density function of $\boldsymbol{Y}$ is given by [25]

$$p_{\boldsymbol{Y}}(\boldsymbol{Y}) = \frac{1}{\Gamma_{N_r}(N_t)}[\det(\boldsymbol{\Psi})]^{-N_t}[\det(\boldsymbol{Y})]^{N_t-N_r}\text{etr}(-\boldsymbol{\Psi}^{-1}\boldsymbol{Y}), \quad \boldsymbol{Y} > 0 \tag{29}$$

where $\Gamma_{N_r}(N_t) = \pi^{N_r(N_r-1)/2}\prod_{j=0}^{N_r-1}\Gamma(N_t-j)$ is the multivariate gamma function and $\Gamma(\cdot)$ is the gamma function. From the density of $\boldsymbol{Y}$, we have

$$\mathbb{E}[\det(\boldsymbol{Y})] = \frac{1}{\Gamma_{N_r}(N_t)}[\det(\boldsymbol{\Psi})]^{-N_t}\int_{\boldsymbol{Y}>0}[\det(\boldsymbol{Y})]^{N_t-N_r+1}\text{etr}(-\boldsymbol{\Psi}^{-1}\boldsymbol{Y})\, d\boldsymbol{Y}. \tag{30}$$

Make the change of variate $\boldsymbol{Y} = \boldsymbol{\Psi}^{1/2}\boldsymbol{Z}\boldsymbol{\Psi}^{1/2}$. With Jacobian $(d\boldsymbol{Y}) = [\det(\boldsymbol{\Psi})]^{N_r}(d\boldsymbol{Z})$, we have

$$\begin{aligned}\mathbb{E}[\det(\boldsymbol{Y})] &= \frac{1}{\Gamma_{N_r}(N_t)}[\det(\boldsymbol{\Psi})]^{-N_t}\int_{\boldsymbol{Z}>0}[\det(\boldsymbol{Z})]^{N_t-N_r+1}[\det(\boldsymbol{\Psi})]^{N_t+1}\text{etr}(-\boldsymbol{Z})\, d\boldsymbol{Z} \\ &= \frac{1}{\Gamma_{N_r}(N_t)}[\det(\boldsymbol{\Psi})]^{-N_t}[\det(\boldsymbol{\Psi})]^{N_t+1}\Gamma_{N_r}(N_t+1) \;=\; \det(\boldsymbol{\Psi})\prod_{j=0}^{N_r-1}(N_t-j).\end{aligned} \tag{31}$$

This completes the proof.

APPENDIX B
PROOF OF PROPOSITION 1

Applying Jensen's inequality to (9) and when SNR is not low, we have

$$C_{\text{CF}} \le W\log_2\mathbb{E}\left[\det\left(\boldsymbol{I} + \frac{P_{st}}{N_0W}\boldsymbol{\Xi}\right)\right] \approx W\log_2\mathbb{E}\left[\det\left(\frac{P_{st}}{N_0W}\boldsymbol{\Xi}\right)\right]. \tag{32}$$

If $\widetilde{\boldsymbol{H}} \sim \mathcal{CN}_{N_r,N_t}(0,\, \boldsymbol{\Psi} \otimes \boldsymbol{I})$, then $\boldsymbol{\Xi} \sim \mathcal{CW}_{N_r}(N_t,\, \boldsymbol{\Psi})$ where $N_t \geq N_r$. Using (8), and denoting the ergodic capacity upper bound as $\widehat{C}_{\text{CF}}$, we thus obtain Proposition 1.

APPENDIX C
PROOF OF PROPOSITION 2

According to (11), obtaining the expression of $\widehat{E}_{\text{CF}}$ boils down to finding an inverse function of $\widehat{C}_{\text{CF}}$ in (13), i.e. finding a solution for $f^{-1}(\widehat{C}_{\text{CF}})$. As $\widehat{C}_{\text{CF}}$ is derived when SNR is not low according to Proposition 1, we consider the case $(G\gamma P_{st} + 2P_{st}) \gg K_t d^{\zeta}\, N_0 W$ in (13). This assumption is reasonable because that when P_{st} is small, the value of E_{CF} is dominated by the circuit power P_{sc} and P_{rc} as shown in (11). In contrast, E_{CF} is more sensitive and needs a more accurate expression when P_{st} is large. Thus when SNR is not low, we have

$$\widehat{C}_{\text{CF}} \approx W \left[2\log_2 \left(\frac{P_{st}}{K_t d^{\zeta}\, N_0 W} \right) + 1 + \log_2 \left(\frac{G\gamma}{G\gamma + 2} \right) \right]. \tag{33}$$

Solving the equation, we obtain

$$P_{st} = f^{-1}(\widehat{C}_{\text{CF}}) = 2^{\frac{S_{\text{CF}}}{2} - \frac{1}{2}} K_t d^{\zeta} N_0 W \sqrt{\frac{G\gamma + 2}{G\gamma}}. \tag{34}$$

Substituting (34) into (11), and let $S_{\text{CF}} = \frac{C_{\text{CF}}}{W}$ we thus obtain (14). Note that the condition of S_{CF} in (14) is due to the power constraint of $0 < P_{st} \leq P_{\text{max,s}}$.

APPENDIX D
PROOF OF CONVEXITY FOR $\widehat{E}_{\text{CF}}(\gamma)$ UNDER SCENARIO I

Note that prove $\widehat{E}_{\text{CF}}(\gamma)$ is concave is equivalent to prove $P_{\text{tot}}(\gamma)$ is convex. According to (14), we have

$$\begin{aligned} \frac{\partial P_{\text{tot}}(\gamma)}{\partial \gamma} &= \frac{\partial}{\partial \gamma} \left[(2\xi_s + \gamma \xi_r) 2^{\frac{S_{\text{CF}}}{2} - \frac{1}{2}} K_t d^{\zeta} N_0 W \sqrt{\frac{G\gamma + 2}{G\gamma}} + 2P_{sc} + P_{rc} \right] \\ &= 2^{\frac{S_{\text{CF}}}{2} - \frac{1}{2}} K_t d^{\zeta} N_0 W \frac{(\xi_r \gamma^2 G + \xi_r \gamma - 2\xi_s)}{\sqrt{\frac{G\gamma+2}{G\gamma}} G\gamma^2}, \end{aligned} \tag{35}$$

where $\frac{\partial}{\partial\gamma}(\cdot)$ denotes the derivative of a function with respect to the variable γ. Then we have the second-order derivative of $P_{\text{tot}}(\gamma)$ with respect to γ

$$\frac{\partial^2 P_{\text{tot}}(\gamma)}{\partial\gamma^2} = \frac{\partial}{\partial\gamma}\left[\frac{\partial P_{\text{tot}}(\gamma)}{\partial\gamma}\right] = 2^{\frac{S_{\text{CF}}}{2}-\frac{1}{2}} K_t d^{\zeta} N_0 W \frac{(6\xi_s - \xi_r\gamma + 4\xi_s G\gamma)}{(G\gamma+2)G\gamma^3\sqrt{\frac{G\gamma+2}{G\gamma}}}. \tag{36}$$

If $\xi_r \leq 4\xi_s G$, we have $\frac{\partial^2 P_{\text{tot}}(\gamma)}{\partial\gamma^2} \geq 0$ on $\gamma \in (0, P_{\text{max,r}}/P_{st}]$. Since the scaling factors ξ_s and ξ_r are always natural numbers and in the same order of magnitude as indicated in [8], and as we are interested in high values of G, it is highly reasonable to assume $\xi_r \leq 4\xi_s G$. Thus we have $\frac{\partial^2 P_{\text{tot}}(\gamma)}{\partial\gamma^2} \geq 0$ and $P_{\text{tot}}(\gamma)$ is convex on $\gamma \in (0, P_{\text{max,r}}/P_{st}]$. This completes the proof that $\widehat{E}_{\text{CF}}(\gamma)$ is a concave function on $\gamma \in (0, P_{\text{max,r}}/P_{st}]$.

APPENDIX E
PROOF OF CONVEXITY FOR $\widehat{E}_{\text{CF}}(\gamma,\phi)$ UNDER SCENARIO II

The EE upper bound $\widehat{E}_{\text{CF}}$ for Scenario II is given by (18), where the function $(1+G\gamma P/\phi)^{\phi}-1$ is strictly increasing on $\gamma \in (0,1]$ and $\phi \in (0,1]$ and can be fitted by polynomial functions. We use a quadratic polynomial $G\gamma P\phi^2$ to fit $(1+G\gamma P/\phi)^{\phi}-1$, so that the total power for the entire system can be manipulated as

$$P_{\text{tot}}(\gamma,\phi) = 2P_{sc}+P_{rc} + \frac{(2\xi_s+\gamma\xi_r)K_t d^{\zeta} N_0 W}{\sqrt{2}G\gamma\phi} \cdot \sqrt{G\gamma(2^{S_{\text{CF}}(1+\phi)}G\gamma\phi^2 + 2^{1+S_{\text{CF}}+S_{\text{CF}}\phi})}. \tag{37}$$

The polynomial fitting preserves the original function's increasing property and helps provide a closed-form solution for P_{tot}. Proving the convexity of $\widehat{E}_{\text{CF}}(\gamma,\phi)$ thus boils down to proving the convexity of $P_{\text{tot}}(\gamma,\phi)$. Based on (37), we have

$$\frac{\partial^2 P_{\text{tot}}(\gamma,\phi)}{\partial\gamma^2} = \frac{2^{-1/2+S_{\text{CF}}+\phi\, S_{\text{CF}}} K_t d^{\zeta} N_0 W\ (-\xi_r\gamma + 4\,G\gamma\phi^2\xi_s + 6\,\xi_s)}{\gamma^2\,(G\gamma\phi^2+2)\,\phi\,\sqrt{G\gamma 2^{S_{\text{CF}}\,(1+\phi)}\,(G\gamma\phi^2+2)}}. \tag{38}$$

Since the scaling factors ξ_s and ξ_r are always natural numbers and in the same order of magnitude as indicated in [8] and we are interested in high values of G, it is highly reasonable to assume $\xi_r \leq 6\xi_s P_{st}/P_{\text{max,r}} + 4\xi_s G\phi^2$. Thus we have $\frac{\partial^2 P_{\text{tot}}(\gamma,\phi)}{\partial\gamma^2} \geq 0$ on $\gamma \in (0, P_{\text{max,r}}/P_{st}]$. In addition,

from (37) we obtain

$$\frac{\partial^2 P_{\text{tot}}(\gamma,\phi)}{\partial \phi^2} = \frac{(2\,\xi_s + \xi_r \gamma)\, K_t d^{\zeta}\, N_0 W\, 2^{1/2+S_{\text{CF}}+S_{\text{CF}}\,\phi}}{8\phi^3\sqrt{Gr 2^{S_{\text{CF}}\,(1+\phi)}\,(G\gamma\phi^2+2)}} \cdot \left[G^2\gamma^2\phi^6 S_{\text{CF}}^2 \ln^2(2) + 4\,G\gamma\phi^4 S_{\text{CF}}^2 \ln^2(2) \right.$$
$$\left. -8G\gamma\phi^3 S_{\text{CF}} \ln(2) + 4\phi^2 {S_{\text{CF}}}^2 \ln^2(2) + 24G\gamma\phi^2 - 16 S_{\text{CF}}\phi \ln(2) + 32\right]. \qquad (39)$$

As high values of G and S_{CF} are more interested, we have $\frac{\partial^2 P_{\text{tot}}(\gamma,\phi)}{\partial \phi^2} \geq 0$ on $\phi \in (0,1]$ as well. Therefore, on the set of $\gamma \in (0, P_{\text{max,r}}/P_{st}]$ and $\phi \in (0,1]$, the Hessian matrix of $P_{\text{tot}}(\gamma,\phi)$ is positive semidefinite [23], and thus $P_{\text{tot}}(\gamma,\phi)$ is a convex function. This completes the proof that $\widehat{E}_{\text{CF}}(\gamma,\phi)$ is concave on $\gamma \in (0, P_{\text{max,r}}/P_{st}]$ and $\phi \in (0,1]$.

ACKNOWLEDGMENT

This work has been done within a joint project, supported by Huawei Tech. Co., Ltd, China. The authors gratefully acknowledge the help of Mr Bernard Hunt for improving the language of the paper.

REFERENCES

[1] R. Dabora and S. D. Servetto, "Broadcast channels with cooperating decoders," *IEEE Trans. Inform. Theory*, vol. 52, no. 12, pp. 5438–5454, Dec. 2006.

[2] C. T. K. Ng, N. Jindal, A. J. Goldsmith, and U. Mitra, "Capacity gain from two-transmitter and two-receiver cooperation," *IEEE Trans. Inform. Theory*, vol. 53, no. 10, pp. 3822–3827, Oct. 2007.

[3] Z. Ding, K. Leung, D. Goeckel, and D. Towsley, "Cooperative transmission protocols for wireless broadcast channels," *IEEE Trans. on Wireless Commun.*, vol. 9, no. 12, pp. 3701–3713, Dec. 2010.

[4] J. Jiang, J. S. Thompson, and H. Sun, "A singular-value-based adaptive modulation and cooperation scheme for virtual-MIMO systems," *IEEE Trans. Vehicular Technology*, vol. 60, no. 6, pp. 2495–2504, July 2011.

[5] J. Jiang, J. Thompson, H. Sun, and P. Grant, "Performance assessment of virtual multiple-input multiple-output systems with compress-and-forward cooperation," *IET Communications*, vol. 6, no. 11, pp. 1456–1465, 2012.

[6] F. Heliot, M. Imran, and R. Tafazolli, "On the energy efficiency-spectral efficiency trade-off over the MIMO Rayleigh fading channel," *IEEE Trans. Communications*, vol. 60, no. 5, pp. 1345–1356, May 2012.

[7] Y. Chen, S. Zhang, S. Xu, and G. Li, "Fundamental trade-offs on green wireless networks," *IEEE Commun. Mag.*, vol. 49, no. 6, pp. 30–37, June 2011.

[8] G. Auer, V. Giannini, C. Desset, I. Godor, P. Skillermark, M. Olsson, M. Imran, D. Sabella, M. Gonzalez, O. Blume, and A. Fehske, "How much energy is needed to run a wireless network?" *IEEE Wireless Communications*, vol. 18, no. 5, pp. 40–49, Oct. 2011.

[9] Y. Chen, S. Zhang, and S. Xu, "Characterizing energy efficiency and deployment efficiency relations for green architecture design," in *2010 IEEE International Conference on Communications Workshops (ICC)*, May 2010, pp. 1–5.

[10] Y. Yao, X. Cai, and G. Giannakis, "On energy efficiency and optimum resource allocation of relay transmissions in the low-power regime," *IEEE Trans. Wireless Commun.*, vol. 4, no. 6, pp. 2917–2927, Nov. 2005.

[11] X. Cai, Y. Yao, and G. B. Giannakis, "Achievable rates in low-power relay links over fading channels," *IEEE Trans. Commun.*, vol. 53, no. 1, pp. 184–194, 2005.

[12] J. Gomez-Vilardebo, A. Perez-neira, and M. Najar, "Energy efficient communications over the AWGN relay channel," *IEEE Trans. Wireless Commun.*, vol. 9, no. 1, pp. 32–37, Jan. 2010.

[13] S. Cui, A. Goldsmith, and A. Bahai, "Energy-efficiency of MIMO and cooperative MIMO techniques in sensor networks," *IEEE Journal on Selected Areas in Commun.*, vol. 22, no. 6, pp. 1089 –1098, Aug. 2004.

[14] S. Jayaweera, "Virtual MIMO-based cooperative communication for energy-constrained wireless sensor networks," *IEEE Trans. Wireless Commun.*, vol. 5, no. 5, pp. 984–989, May 2006.

[15] Y. Qi, R. Hoshyar, M. Imran, and R. Tafazolli, "H2-ARQ-relaying: Spectrum and energy efficiency perspectives," *IEEE Journal on Selected Areas in Communications*, vol. 29, no. 8, pp. 1547–1558, Sep. 2011.

[16] D. Tse and P. Viswanath, *Fundamentals of Wireless Communication*. New York, NY, USA: Cambridge University Press, 2005.

[17] G. Auer and et al., "D2.3: Energy efficiency analysis of the reference systems, areas of improvement and target breakdown," INFSO-ICT-247733 EARTH (Energy Aware Radio and NeTwork TecHnologies), Tech. Rep., Nov. 2010.

[18] Y. Qi, M. A. Imran, D. Sebella, B. Debaillie, R. Fantini, and Y. Fernandez, "Deployment opportunities for increasing energy efficiency in LTE-advanced with relay nodes," in *29th Meeting of WWRF*, 2012, pp. 1–5.

[19] Y. Liang, V. V. Veeravalli, and H. V. Poor, "Resource allocation for wireless fading relay channels: Max-min solution," *IEEE Trans. Inform. Theory*, vol. 53, no. 10, pp. 3432–3453, Oct. 2007.

[20] A. Host-Madsen and J. Zhang, "Capacity bounds and power allocation for wireless relay channels," *IEEE Trans. Inform. Theory*, vol. 51, no. 6, pp. 2020–2040, June 2005.

[21] I. Krikidis, J. Thompson, S. McLaughlin, and N. Goertz, "Optimization issues for cooperative amplify-and-forward systems over block-fading channels," *IEEE Trans. on Vehicular Technology*, vol. 57, no. 5, pp. 2868–2884, Sept. 2008.

[22] T. T. Kim, M. Skoglund, and G. Caire, "Quantifying the loss of compress-forward relaying without Wyner-Ziv coding," *IEEE Trans. Inform. Theory*, vol. 55, no. 4, pp. 1529–1533, April 2009.

[23] S. Boyd and L. Vandenberghe, *Convex Optimization*. Cambridge University Press, 2004.

[24] L. Zhang, Y. Xin, Y.-C. Liang, and H. Poor, "Cognitive multiple access channels: optimal power allocation for weighted sum rate maximization," *IEEE Transactions on Communications*, vol. 57, no. 9, pp. 2754 –2762, Sep. 2009.

[25] A. K. Gupta and D. K. Nagar, *Matrix Variate Distributions*. Boca Raton, Fla, USA: Chapman & Hall/CRC, 2000.

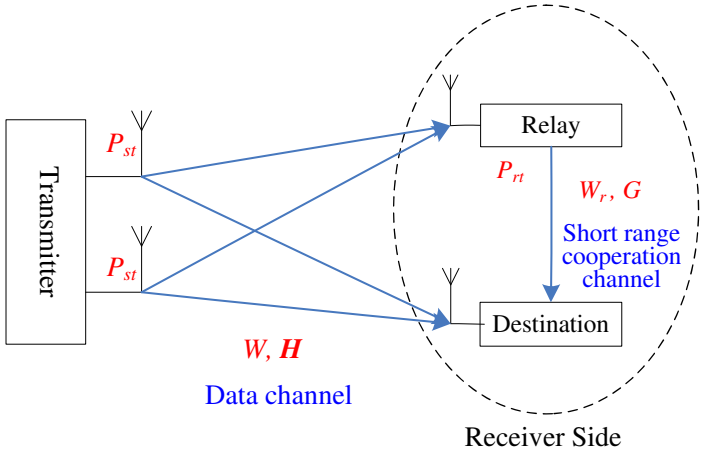

Fig. 1. System model of the virtual-MIMO system ($N_t = N_r = 2$)

TABLE I
OPTIMIZATION ALGORITHM FOR (27) UNDER BANDWIDTH SCENARIO II

Initialize: $k = 0$, $\rho^{(0)}$, $\mu^{(0)}$, $\gamma^{(0)}$, and $\phi^{(0)}$.

Repeat

(a) Obtain the possible optimal values $\gamma^{\dagger}(\rho^{(k)}, \mu^{(k)})$ and $\phi^{\dagger}(\rho^{(k)}, \mu^{(k)})$ by solving $\dfrac{\partial E_{\mathrm{CF}}(\gamma, \phi)}{\partial \gamma}\Big|_{\phi=\phi^{(k)}} = \rho^{(k)}$ and $\dfrac{\partial E_{\mathrm{CF}}(\gamma, \phi)}{\partial \phi}\Big|_{\gamma=\gamma^{(k)}} = \mu^{(k)}$, where $E_{\mathrm{CF}}(\gamma, \phi)$ is giving by (18).

(b) Update the parameters $\gamma^{(k)}$, $\phi^{(k)}$, $\rho^{(k+1)}$, and $\mu^{(k+1)}$ by

$$\begin{cases} \gamma^{(k)} = \gamma^{\dagger}(\rho^{(k)}, \mu^{(k)}), & \phi^{(k)} = \phi^{\dagger}(\rho^{(k)}, \mu^{(k)}); \\ \rho^{(k+1)} = \left[\rho^{(k)} - \tau_1^{(k)} g_1^{(k)}\right]^+, & \mu^{(k+1)} = \left[\mu^{(k)} - \tau_2^{(k)} g_2^{(k)}\right]^+. \end{cases}$$

(c) Calculate the Lagrangian function $L(\gamma^{(k)}, \phi^{(k)}, \rho^{(k)}, \mu^{(k)})$.

(d) $k = k + 1$.

Until: Lagrangian function $L(\gamma^{(k)}, \phi^{(k)}, \rho^{(k)}, \mu^{(k)})$ converges to a preset tolerance.

Output: The final optimal values $\gamma^{\dagger}$ and $\phi^{\dagger}$.

TABLE II
SIMULATION PARAMETERS (VALUES OF POWER MODEL PARAMETERS ARE SUGGESTED BY [8] AND [18]).

Parameter	Value	Parameter	Value
N_0	-174 dBm/Hz	P_{sc}(Macro)	130 W
W	10 MHz	ξ_s(Macro)	4.7
K_t	10^{-3}	$P_{\text{max,r}}$(relay)	5 W
d	500 m	P_{rc}(relay)	14.3 W
ζ	3.5	ξ_r(relay)	2.8
$P_{\text{max,s}}$(Macro)	20 W		

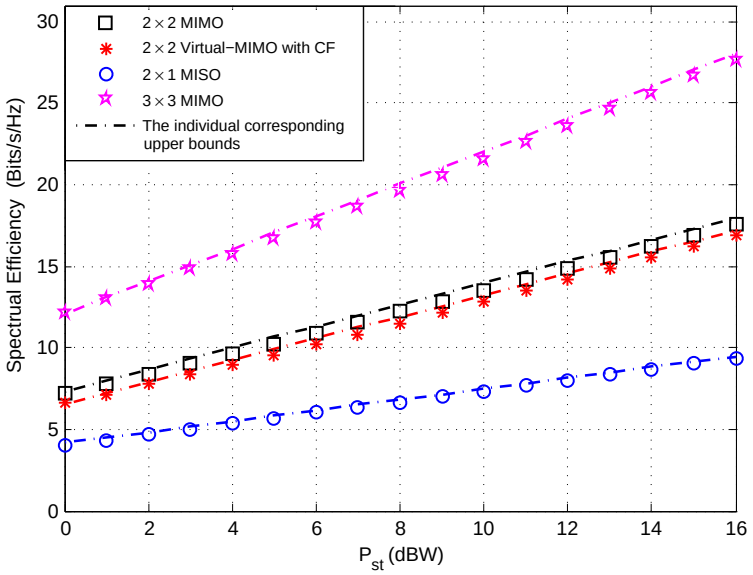

Fig. 2. Simulation results and upper bounds of the ergodic capacity for $N_t \times N_r$ MIMO and virtual-MIMO systems. (For virtual MIMO, $G = 10$ dB and $\gamma = 0.25$ are considered; For virtual MIMO using CF, bandwidth Scenario I is considered.)

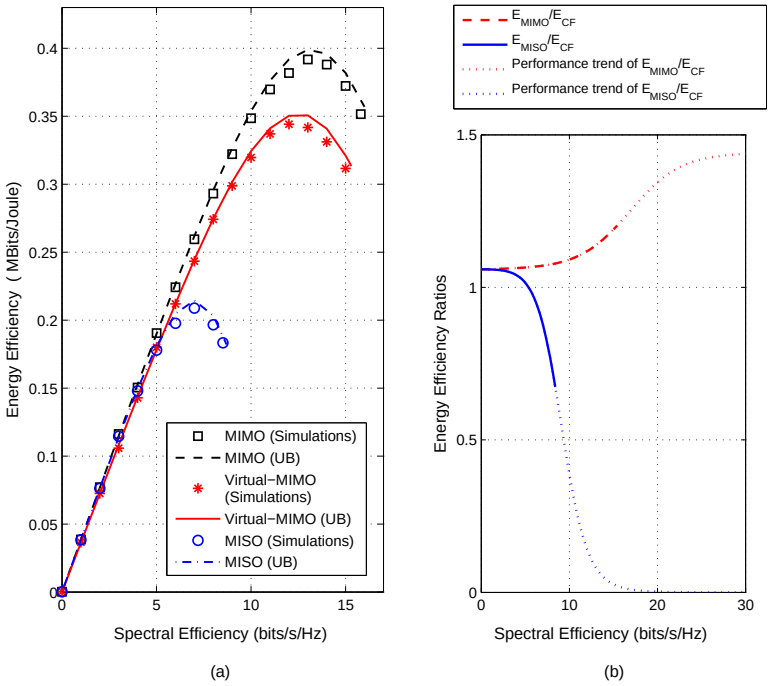

Fig. 3. EE performance of virtual-MIMO with CF for bandwidth Scenario I, compared with those of MISO and MIMO systems. (For virtual MIMO, $G = 10$ dB and $\gamma = 0.25$ are considered.)

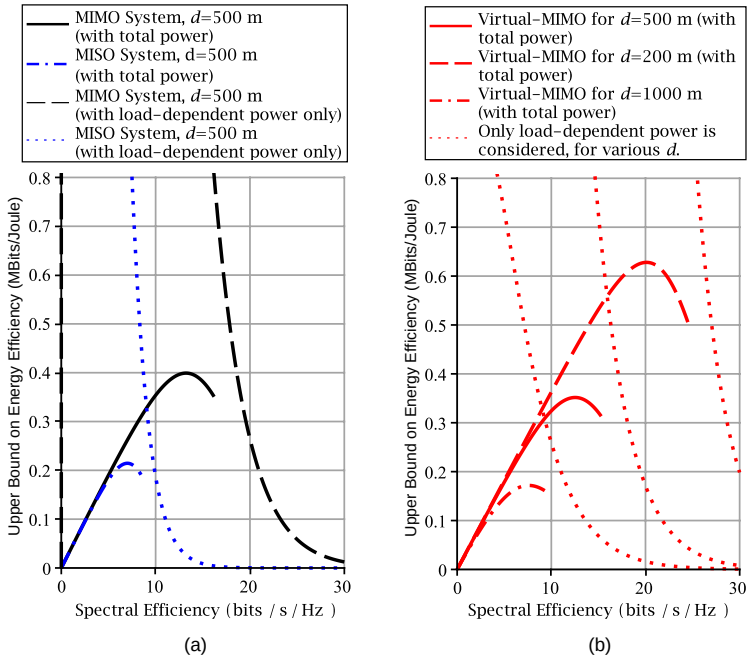

Fig. 4. The effects of load-dependent power on the overall EE performance under bandwidth Scenario I (The performance of MIMO and MISO systems are shown in (a), and that of virtual-MIMO using CF and considering $G = 10$ dB and $\gamma = 0.25$ is in (b).)

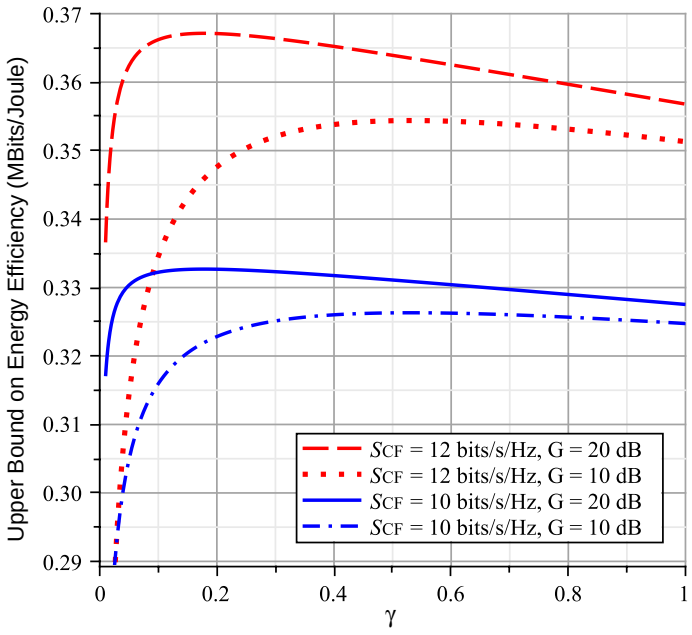

Fig. 5. The effects of varying the values of γ on the EE performance of the virtual-MIMO system with CF by setting $S_{\text{CF}} = 10, 12$ bits/s/Hz and $G = 10, 20$ dB under bandwidth Scenario I.

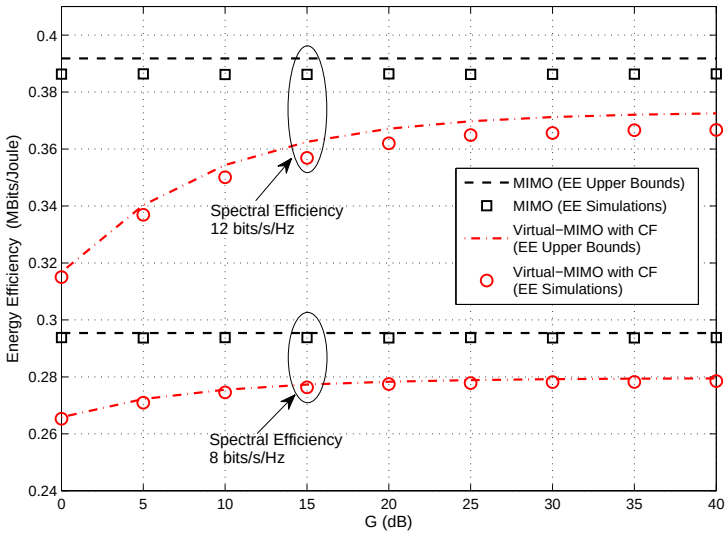

Fig. 6. EE comparisons between virtual-MIMO with CF and ideal MIMO against the cooperation channel power gain G with SE = 8, 12 bits/s/Hz under bandwidth Scenario I. (For virtual MIMO, optimal power allocation is performed.)

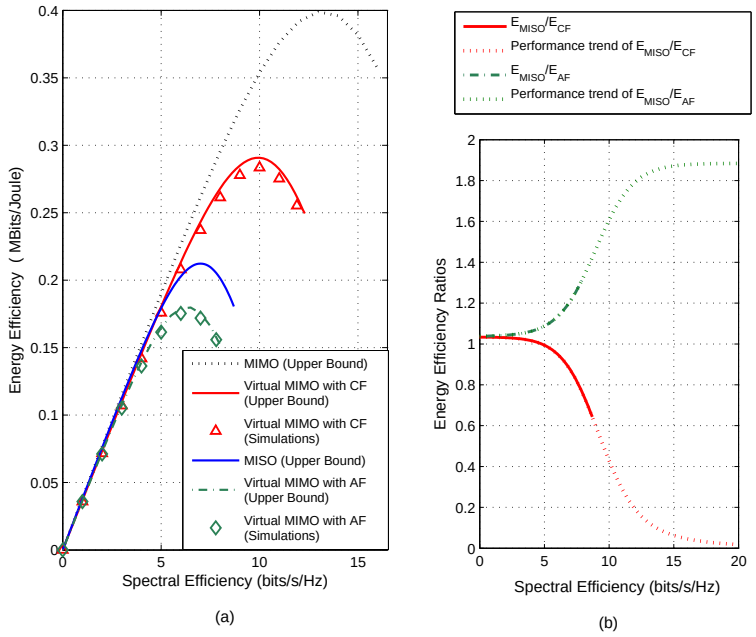

Fig. 7. EE performance of the virtual-MIMO system under bandwidth Scenario II with setting $G = 20$ dB. (Optimal power allocation is performed for the AF case, while optimal joint power and bandwidth allocation is performed for CF.)

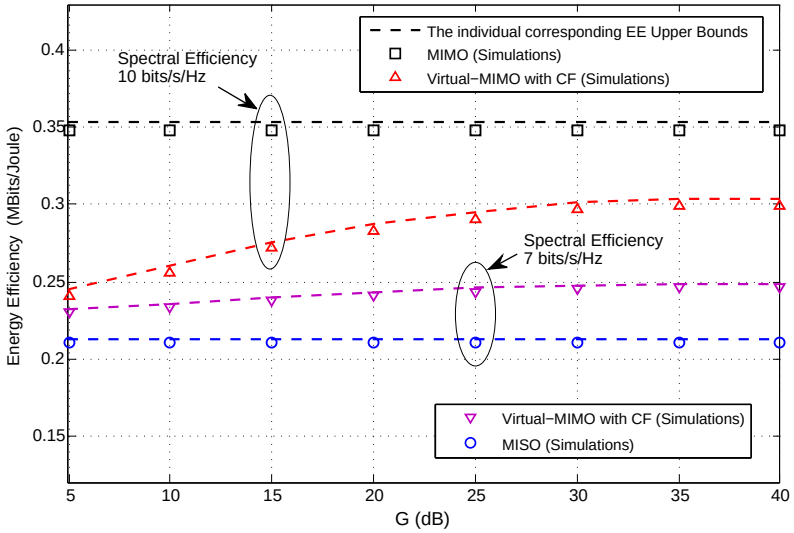

Fig. 8. EE comparisons among virtual-MIMO, ideal MIMO, and MISO against the cooperation channel power gain G with SE = 7, 10 bits/s/Hz under bandwidth Scenario II. (Optimal joint power and bandwidth allocation is performed for CF.)